Published in final edited form as:

Biomed Mater. ; 13(3): 035013. doi:10.1088/1748-605X/aaaa29.

Self-neutralizing PLGA/Magnesium Composites as Novel Biomaterials for Tissue Engineering

Thomas O. Xu[1], **Hyun S. Kim**[2], **Tyler Stahl**[2], and **Syam P. Nukavarapu**[1,2,3]

[1]Department of Orthopaedic Surgery, University of Connecticut Health Center, Farmington CT

[2]Department of Biomedical Engineering, University of Connecticut, Storrs CT

[3]Department of Material Science & Engineering, University of Connecticut, Storrs CT

Abstract

Controlling acidic degradation of biodegradable polyesters remains a major clinical challenge. This work presents a simple and effective strategy of developing polyester composites with biodegradable magnesium metal or alloys. PLGA samples with compositions of 1, 3, 5, and 10 wt % magnesium were simply produced using the solvent-casting method, which resulted in composite films with near uniform Mg metal/alloy particle dispersion. Degradation study of the composite films showed that all compositions higher than 1 wt% magnesium were able to extend the duration of degradation, and buffer acidic pH resulting from PLGA degradation. PLGA composite with 5 wt% of magnesium is found to show near-neutral degradation pattern in sink condition. Magnesium addition also showed improved mechanical characteristics in terms of the tensile modulus and strength. *In vitro* experiments conducted by seeding PLGA composites with MC3T3-E1 pre-osteoblasts demonstrated increased ALP expression, and cellular mineralization. The established new biodegradable polymer-metal system provides a useful biomaterial platform with a wide range of applications in biomedical device development and scaffold-based tissue engineering.

Keywords

Magnesium; Magnesium Alloys; Biodegradable metal/alloy; Polyesters; Neutral degradation; Bio-mineralization; Biocompatibility

1. Introduction

Biomaterials of natural and synthetic origin have been developed for biomedical applications, including tissue engineering [1]. Synthetic biomaterials include polyesters, polyurethanes, polyanhydrides, polyamides and polyphosphazenes [2, 3]. Among these, polyesters have received wide attention as biodegradable biomaterials to develop biomedical implants as well as three-dimensional and porous scaffold systems for tissue engineering applications [4–12].

Biodegradable polyesters are attractive due to their excellent biocompatibility and tunable physico-chemical properties. For example, PLGA co-polymer's mechanical and degradation characteristics can be fine-tuned by varying lactic acid to glycolic acid ratio [13, 14]. Based

on the initial success, some polyesters have received FDA approval to be part of biomedical devices, such as biodegradable sutures and orthopedic fixation devices [4, 15, 16]. However, polyester (PGA, PLLA, and PLGA) degradation results in acidic by-products [17, 18]. This leads to acid build-up, which is reported to cause local inflammation, infection and eventually may lead to implant failure [19–21].

To specifically address polyester acidic degradation, composite, and blend strategies are employed. In the composite strategy, polyesters are combined with inorganic phosphates such as calcium phosphate or hydroxyapatite, using the biocompatibility and tunable mechanical properties of bone-like biomaterials. For example, tricalcium phosphate (TCP) has been shown to buffer the acidic degradation of PLGA, by hindering the degradation of PLGA and its autocatalysis [22, 23]. However, PLGA composited with hydroxyapatite did not display significant buffering capabilities [24, 25]. Polymer-polymer blends have also been formed by combining PLGA or PLA with polymers that produce products of basic nature, such as polyphosphazene and other amino acid-derived polymers. This strategy also developed a number of biomaterial compositions with tunable physical and biological properties [26–30]. Both these approaches were successful in terms of creating new biomaterial compositions, however failed to produce polyester biomaterials with neutral degradation products.

Recently, biodegradable metals (Mg, Zn and Fe) and alloys have been developed as an alternative to biodegradable polymers as biomaterials [31]. Among those, magnesium (Mg) and its alloys have attracted attention due to lightweight, bone like mechanical properties, and osteoconductive properties, along with the fact that Mg is already prevalent within the body. [32–36]. Additionally, Mg is essential to bone metabolism and enzymatic reactions in the body. Uncontrolled degradation and hydrogen gas production are the chief concerns associated with Mg alone as a biomaterial. However, these concerns are mitigated by alloying Mg with other metals such as Al and Zn [32, 37, 38].

In this work, we propose to develop self-neutralizing polymer/metal composite biomaterials by combining PLGA with Mg metal/alloys. It is known that magnesium or magnesium alloys produce magnesium hydroxide, which is basic (pH>7), upon degradation. Therefore, it is hypothesized that the basic degradation product of the Mg metal or alloy will buffer the acidic degradation of the PLGA. Additionally, the PLGA matrix will serve to slow down corrosion of the Mg particles. Through forming PLGA/Mg composites, we expect to develop a new class of biomaterials with synergistically improved physico-chemical as well as biological properties. In this manuscript, a series of PLGA-Mg metal/alloy composite biomaterials were reported and investigated the effect of Mg metal/alloy addition on PLGA degradation and biocompatibility.

2. Materials and Methods

2.1 PLGA/Mg Composite Preparation

PLGA, PLGA-Mg, and PLGA-ZK61 composite films were fabricated using a solvent casting method [28, 30] followed by drying. Briefly, 1.0 g of PLGA 85/15 (Lakeshore Biomaterials) was dissolved in dichloromethane (Fisher Scientific) in a ratio of 1:5 g:mL.

Pre-calculated amounts of pure Mg or Mg-Zn Alloy (ZK61; 94.5% Mg, 5% Zn, TangShan WeiHao Magnesium Powder Co. China) powder (40 μm average diameter) were added to the polymer solution to form composites with 1, 3, 5, and 10 wt% Mg metal or Mg-Zn alloy. The solution was vortexed for 30 min before casting into a 150 mm polystyrene petri dish lined with Bytac® paper and left to air dry for 24 hours at 4°C. After the solvent evaporation, the films were dried for 24 hours at room temperature and stored in a desiccator until use. Films were bored into 12 mm diameter circles and 20 mm long and 7 mm width strips. The circular samples were used for degradation, biomineralization and cell studies while the strips were used for mechanical testing.

2.2 Mechanical Characterization

Tensile testing of the PLGA and PLGA-Mg composite films (0.2 mm thick, 70 mm long and 7 mm width, n=6/group) was performed at a rate of 2mm/min with 20 mm initial grip separation (Instron 5544, Instron Corp., MA) following the standard protocol of ASTM D882 [39]. In brief, the samples were elongated by 10 mm (in addition to the original length) and the corresponding stress strain values were recorded. The tensile strength and modulus were calculated based on the recorded stress-strain data using the associated software, Bluehill 3.

2.3 Degradation

To assess the ability of Mg to buffer and slow the degradation of a PLGA matrix, 12 mm diameter films were completely submerged and degraded in 10 mL of phosphate buffered saline (PBS) at 47°C. The groups tested consist of PBS control, pure PLGA (85:15), and composite films PLGA-Mg and PLGA-ZK61 composed of 1, 3, 5, and 10% Mg or ZK61 Mg-Zn alloy. Elevated temperatures have been shown to accelerate PLGA degradation [40–42], and 47°C was used to obtain a reasonable timeframe for the experiment. The pH was measured once every two days until the films were completely degraded. To simulate the *in vivo* conditions (degradation product clearance through diffusion), the degradation studies were also done under sink condition, where the degradation media was replaced with fresh PBS once in 7 days. The solution pH was measured before each media change to capture true pH change within the time period. The measurement is followed with a reset of pH to 7.4 by replenishing with fresh PBS. PLGA and PLGA-Mg composites with 5 wt% of Mg were studied for degradation using the sink conditions.

2.4 Biomineralization analysis

To assess the effect of Mg addition and concentration on mineral deposition, the PLGA-Mg films with compositions of 0, 1, 3, 5, and 10 % w/w were subjected for biomineralization in vitro. The films were immersed in 15 mL of 1.5× simulated body fluid (SBF) to expedite the mineralization and kept at a constant temperature of 37 °C. Samples were removed after 14 days, and the SBF solution was refreshed every 2 days. The SBF was prepared using a well-established protocol [43, 44] and all chemicals used for the preparations were obtained from Sigma-Aldrich, MO.

Post-biomineralization, the samples were rinsed with double distilled water to remove remaining SBF and air-dried. The dried samples were then sputter coated with gold/

palladium (E5100, Polaron) and examined using a scanning electron microscope (Nova NanoSEM 450, FEI). X-ray Energy Dispersive Spectroscopy (EDS) was also performed using Oxford Aztec Energy Microanalysis System with X-Max 80 Silicon Drift Detector to determine the atomic compositions of calcium apatites formed during the process. The atomic compositions from EDS were roughly quantified to a Ca:P ratio to determine the effect of Mg on the apatite composition formed.

2.5 In vitro evaluation

To assess the ability of the composite films to support cell compatibility and osteoconduction, MC3T3-E1 mouse pre-osteoblast cells were seeded onto films and cultured for 21 days in vitro. For these studies, the samples were sterilized in 70% ethanol and exposed to UV radiation on both sides for 15 minutes each prior to cell culture. Sterilized 5% PLGA-Mg and 5% PLGA-ZK61 composite films were seeded with a total of 25,000 cells and cultured in standard *in vitro* osteoblast differentiation media (α-minimal essential medium, 10% fetal bovine serum, 1% penicillin/streptomycin, 10 nM Dexamethasone, 50 μg/mL ascorbic acid, and 10 mM β-glycerophosphate) in 48-well tissue culture plates, and kept at 37°C and 5% CO_2, replacing the media every 2-3 days.

2.6 Cell Proliferation

Cell proliferation was quantitatively analyzed using a fluorescent dsDNA assay (Quanti-iT PicoGreen dsDNA assay, Invitrogen) as described in previous work [45]. At days 1, 7, 14, and 21, cellularized films were taken out of culture and washed with PBS. Cells were then permeabilized with 1mL of 1% Triton X-100 for 30 minutes and run through three freeze-thaw cycles at -70°C and room temperature, respectively. Subsequently, Quanti-iT PicoGreen reagent was added to each well and incubated at room temperature for 10 minutes. The plates were then measured for fluorescence at 485 nm/535 nm using a Synergy HT plate reader (BioTek Instruments, Inc., Vermont). The measured fluorescence was used in accordance with the standard curve constructed using standard λ-DNA to quantify the DNA content of the lysate.

2.7 Alkaline Phosphatase (ALP) Activity

Alkaline phosphatase activity of cells cultured on the films was colormetrically analyzed using an ALP substrate kit (Bio-Rad) as mentioned in previous work [3]. The same cell lysate from days 1, 7, 14 and 21 from the cell proliferation assay were used to analyze ALP activity. In brief, 100 μL of a p-nitrophenyl phosphate (p-NPP) solution was added to 25 μL cell lysate and incubated at 37°C for 30 min to allow ALP to convert p-NPP into p-nitrophenol (p-NP). The reaction was stopped using 125 μL of 0.4M NaOH. The plates were then read for absorption at 405 nm using a plate reader and normalized with corresponding DNA concentration of the lysate.

2.8 Mineralization Assay

Mineralized matrix synthesis by the seeded cells was evaluated using alizarin red staining and calcium quantification protocol used in previous work [6]. Colorimetric analysis is based on the solubility of the alizarin red-matrix complex solubility in a cetylpryidinium

chloride (CPC, Sigma Aldrich) solution. Briefly, at days 14 and 21 cellularized composite films were washed with distilled water and fixed with 70% ethanol at 4°C for 20 minutes. The ethanol was then removed and allowed to air-dry. Samples were then covered and incubated with alizarin red dye (pH 4.23, Sigma Aldrich) for 10 minutes at room temperature. Samples were washed multiple times with distilled water to remove excess alizarin red dye and washed once with PBS before solubilizing the dye-matrix complex. 10% (w/v) CPC was added to the samples to solubilize the dye-matrix complex and allowed to incubate for 15 minutes at room temperature. Acellular film for each group was used as an internal control. The plates were then read for absorption at 562 nm using a TECAN plate reader.

2.9 Statistical Analysis

For mechanical strength data analysis, one-way analysis of variance (ANOVA) was used followed by Tukey's Multiple Comparison Test. For cell proliferation, ALP activity, and mineralization analysis, a two-way analysis of variance (ANOVA) was performed to compare data. Error is reported in figures as standard deviation and significance was reported using a probability value of $p < 0.050$

3. Results

3.1 Magnesium particle distribution

Magnesium particle dispersion in PLGA-Mg films were imaged under a bright field optical microscope for particle dispersion. Optical micrographs recorded for composites with Mg content 1, 3, 5, and 10 wt% are shown in Figure 1. For lower Mg content, composite films displayed relatively homogeneous particle distribution. As the Mg content increased from 1 to 10% there seemed some level of particle agglomeration, which is evident with the 10% Mg loading, as shown in Figure 1. Based on this observation, the current study limits Mg loading up to 10 wt%.

3.2 Mechanical Reinforcement

In order to assess mechanical reinforcement from the dispersed Mg metal/alloy particles, PLGA-Mg composites were subjected for mechanical strength measurements in tensile mode. As shown in Figure 2, there is a general increasing trend with increasing the amount of Mg content. The increase in modulus is not significant for the lower levels of Mg (1-3 wt %). A significant increase in modulus was seen for the 5 and 10% Mg compositions in comparison to the rest of the groups, with 35-40% increase in modulus compared to PLGA. These results evidence mechanical property tunability by altering the amount of Mg loaded.

3.3 PLGA acidic by-product neutralization

Through pH monitoring of the degradation solution, it was observed that addition of pure Mg or Mg ZK61 alloy could reduce the rapid changes in pH displayed by the PLGA-only films (Figure 3) and allow for the neutralization of the acidic degradation of PLGA. For PLGA-only films, a large drop in pH was observed after 3 weeks of degradation, and the film was fully degraded in about 6 weeks. In contrast, PLGA-Mg composite samples

displayed an initial increase in pH, which was stabilized around pH 7 about a week into the degradation, while the increase in pH was varied based on the Mg composition.

The 1% PLGA-Mg sample displayed a similar degradation profile to the PLGA sample and only showed a small initial increase in pH. The 1% PLGA-Mg sample also fully degraded in about 6 weeks and reached a final degradation solution pH of 2.607 ± 0.026. On the other hand, the 10% PLGA-Mg composite took twice as long to fully degrade and reached a final pH of 3.943 ± 0.045. This sample showed the greatest initial increase in pH, but did not display a rapid pH decrease after the initial increase, exhibiting markedly slower decrease in pH than the 1% PLGA-Mg samples. Each increase in Mg concentration resulted in a slower decline in pH and slower degradation rate (Figure 3). Composite films composed of ZK61 alloy also displayed a trend similar to that of the PLGA-Mg composites.

In a follow up study, the degradation media was replaced every 7 days, referred to as sink condition, to simulate the body fluid circulation and waste removal. The PLGA- 5wt% Mg samples were chosen for further study due to its neutral degradation profile and improved tensile modulus. The study displays an initial increase in pH and a nearly neutral degradation profile, as shown in Figure 4. Comparatively, the PLGA sample displayed much larger swings in pH, with each sharp increase in pH corresponding to replacement of the degradation media (Figure 4). It is important to note that the observed swings in the case of PLGA are absent with composites due to Mg buffering capacity of the PLGA acidic degradation products.

3.4 Effect of Mg addition on PLGA bio mineralization

Biomineralization studies of PLGA-Mg films were conducted to assess the ability to nucleate hydroxyapatite when placed in a simulated physiological environment, using 1.5 × SBF. SEM images recorded after 14 days of biomineralization show mineral nucleation and growth for PLGA and composite films (Figure 5). The mineral deposits ranged from isolated crystals less than 10 μm in diameter seen in PLGA-only samples to the large aggregates and coating seen in the 5 and 10% PLGA-Mg samples. The isolated crystals displayed a spherical morphology with plate-like microstructure, evident on the surface of the crystals, that eventually fused together to form the aggregates seen in the samples with higher Mg content. Furthermore, it was observed that the composites with higher Mg content displayed greater amounts of mineral deposition.

The samples were further analyzed using EDS to determine the deposited mineral composition. The calcium to phosphate ratio was used to confirm whether the mineral formed is hydroxyapatite. As shown in Figure 6, the Ca:P ratios were found to be between 1.539-1.766, with no significant difference between the groups and no obvious trend in Ca:P ratio was observed. Also since the Ca:P ratio of pure hydroxyapatite is 1.667, and the inherent imprecisions of EDS as quantitative data, the deposits were believed to be hydroxyapatite. The EDS was further used to provide spatial distribution of the hydroxyapatite. Calcium and phosphorous mapping recorded for PLGA and PLGA-5wt% Mg are presented in Figure 7. It was found that for the composites, calcium and phosphorous presence coincided precisely with the presence of Mg atoms, indicating Mg induced biomineralization.

3.5 PLGA-Mg Composite osteocompatibility evaluation in vitro

The quantitative cell proliferation and normalized ALP expression are shown in Figure 8. Cell proliferation remained low on day 1 and 7 until a significant rise by day 14. On day 14 and 21, Figure 8A, the number of cells on both the PLGA-Mg and ZK61 films were significantly higher than the number of cells on the pure PLGA films. There was no significant difference in number of cells between the three groups on day 1 and 7. Additionally there was no significant growth in cell number between days 14 and 21 for all samples. On day 14 and 21, Figure 8B, the ALP expression, normalized to cell proliferation, on both the PLGA-Mg and ZK61 Mg alloy films was significantly higher when compared to the pure PLGA film, and very little ALP expression was seen from the cells cultured on pure PLGA films. Additionally, there was a significant increase in ALP expression on both the Mg and ZK61 films between day 14 and 21. There was no significant differences in cell proliferation and ALP activity between the Mg and ZK61 films.

The cellular performance assessed by mineralization is shown in Figure 9. Cells cultured on the Mg and ZK61 films displayed significantly more mineralization when compared to the PLGA counterpart on both day 14 and 21 samples. Additionally, a near two-fold increase in cell mineralization was seen on the Mg films between day 14 and day 21, while no increase in mineralization was seen on the pure PLGA films. The PLGA-ZK61 composite films also showed an increase in mineralization between day 14 and 21, but to a smaller degree when compared with the PLGA-Mg films. Finally, there was no significant difference observed between the Mg and ZK61 films.

4. Discussion

The current study aimed to improve the performance of biodegradable polyesters, in particular PLGA, by forming composites with biodegradable Mg metal or alloys. Mg was chosen as suitable filler as it is a biocompatible metal that degrades into magnesium hydroxide in water, which is basic in nature, and has been shown to be osteogenic previously [46–48]. We developed PLGA composites with Mg and Mg alloy and examined the effectiveness of the filler in improving PLGA mechanical strength, degradation characteristics, and the osteogenic properties.

Pure Mg, when composited with PLGA, increased the tensile modulus of the PLGA films. Tensile modulus increased as the particle loading increased, with a significant increase in tensile modulus at a particle loading of 5%. It is possible that a critical concentration of particles was reached at 5% loading that resulted in a significant increase in modulus. Increased composite strength may be attributed to the inclusion of heterogeneously dispersed solid particles. The inclusion of solid particles is expected to retard fracture propagation by dispersing shear forces within the matrix [49–51]. Therefore, we suggest that at 5% particle loading, the concentration of Mg particles is sufficient enough to disperse a shear force when applied.

We proposed that the formation of the basic $Mg(OH)_2$ through the degradation of Mg will react with the acidic byproducts of PLGA, lactic acid and glycolic acid, resulting in pH neutralization and slow down the degradation of the films. Accordingly, increased particle

loading was shown to extend the period of time that the surrounding medium remained at a near neutral pH, while displaying an initial increase in pH. The initial increase in pH observed with the composite films may be attributed to the initial degradation of exposed magnesium metal/alloy particles, as they spontaneously react with water and produce magnesium hydroxide, which is basic in nature. Subsequent neutralization was then observed due to the acidic degradation of PLGA. The rate of the drop in pH though was lowered for the composite films, most likely due to the presence of the buffering Mg degradation. In addition, samples with higher particle loading took longer to completely degrade, with 10% Mg and ZK61 composites taking nearly double the degradation time in comparison to control PLGA samples. With PLA and PLGA, it is known that decrease in pH accelerates degradation through the low pH initiated degradation or autocatalysis [52–55]. Our degradation data confirms that by adding Mg metal or alloy we could keep pH closer to 7, which reduces the possibility of autocatalysis and enhanced degradation. Therefore, by adding Mg or Mg alloys, we were able to neutralize acidic degradation, and extend the degradation time and this could be used as an effective strategy to tailor PLGA degradation time as needed.

The buffering effect of the incorporated Mg was also demonstrated using a sink condition to simulate dynamic conditions (nutrient supply and waste removal) in the body. 5% Mg films were chosen since they displayed the most neutral degradation profile as per the general degradation results presented in Figure 3. In the sink condition study, we observed that the presence of Mg allowed for the maintenance of a near neutral local environment, which was not the case with the PLGA only samples. Therefore, when taking the body dynamic conditions into consideration, the Mg strategy is proven to be effective in neutralizing the PLGA produced acidic degradation products and maintaining a more neutral degradation profile as seen in Figure 4. We also observed the formation of pore-like structures and bubbles as it was degrading which can mostly likely be attributed to the evolution of hydrogen gas, which is a by-product of the Mg reaction with water. Keeping this in mind, we also included Mg alloy, ZK61, composition in our investigation, which is reported to release less amount of hydrogen gas compared to Mg metal [32, 37].

Immersion of the PLGA-Mg composite films in SBF was used to study their biocompatibility via biomineralization. SBF has been used previously to simulate in vivo bioactivity, specifically for bone regeneration, as calcium apatite precipitation during immersion has been correlated with the material possessing osteoconductive properties [32, 56]. As shown in Figure 5, increased mineralization was seen with increasing Mg content, suggesting improved bioactivity of the composites. The precipitation of calcium apatites has been seen previously when Mg and its alloys were immersed in SBF, which is reported to be due to the increase in local ionic charge near the surface with the degradation of Mg. This is expected to result in the migration and nucleation of ionic components of calcium apatites [57, 58]. The distribution of Mg atoms seen in Figure 7 also suggests the incorporation of Mg^{2+} in the calcium apatite nucleates, most likely in the place of Ca^{2+}, suggesting the increased mineralization was caused by the Mg in the film, as reported in the literature [48, 58]. Overall, the increased mineralization suggest that addition of Mg makes the film more bioactive and favorable for osteogenesis through development of calcium apatite when

exposed to the physiological solution after implantation, which was evidenced previously when Mg alloys were implanted *in vivo* [59].

Both the Mg and Mg alloy scaffolds outperformed the control PLGA film in cell proliferation, cell mineralization, and ALP activity. There was a significant increase in cell proliferation on day 14 for the Mg and ZK61 samples (Figure 8A). Between day 14 and 21 however, no significant increase in cell proliferation was seen, which may be attributed to the differentiation of the cell population. Evidence of cell differentiation is corroborated by the ALP expression and mineralization data (Figure 8B, 9). Levels of ALP expression and mineralization, well-known markers of osteogenic differentiation, rose significantly from day 14 to 21 for the Mg and ZK61 films while the cell proliferation remained relatively stagnant. Furthermore, the cells on the Mg and ZK61 films displayed greater differentiation compared to the cells on the pure PLGA films, presumably due to the osteogenic properties of the Mg metal/alloy. Overall, the data supports our hypothesis that the inclusion of Mg and ZK61 particles can enhance cell growth and differentiation on the composite films. The increased cell proliferation and differentiation is also demonstrated in other studies [46, 60, 61]. While there is no agreed mechanism behind the observed enhancement in bone growth surrounding Mg orthopedic fixtures [61] the presence of local Mg and Mg alloys is reported to increase the amount of intracellular Mg ions thereby increasing intracellular signaling within the surrounding MSCs and osteoprogenitors. It is well known that Ca^{+2} ions contribute to osteogenic differentiation [62–64]. Mg is a bivalent cation like Calcium and we suggest that Mg also may contribute to the process similar to Ca.

Although Mg has relatively low corrosion resistance compared to the conventionally used metals, by creating a composite with PLGA, the degradation of Mg was slowed and was able to continuously buffer the degradation of PLGA for the entire length of the study under sink conditions. However, the degradation of Mg to basic $Mg(OH)_2$ and hydrogen gas which can form gas pockets within the tissue if degradation is left unchecked, was not addressed in this study, yet we believe that the small amounts of Mg used in the current study will not produce significant amounts of H_2 gas as the samples degrade. In addition, there are other methods available to reduce H2 gas production, such as alloying Mg with other metals such as Al and Zn.

5. Conclusions

Through this study, we developed a biodegradable polymer-metal composite system as a new biomaterial platform. By forming PLGA composites with magnesium metal/alloy, we were able to develop self-neutralizing PLGA biomaterial and this strategy could be easily extended to other biodegradable polyesters. In addition, the mechanical strength of PLGA was increased with the addition of magnesium particles, suggesting tunable mechanical properties with respect to the magnesium metal/alloy content. Furthermore, the magnesium addition enhanced cellular proliferation, osteogenic differentiation, and matrix production. In conclusion, we have developed a new composite biomaterial platform with tunable physico-chemical and improved biological properties. Overall, this study established self-neutralizing polyesters that could be potentially developed into safe and biodegradable implants and tissue engineering scaffolds.

Acknowledgments

The authors acknowledge support from AO Foundation, Musculoskeletal Transplant Foundation and NSF (EFRI and AIR). Dr. Nukavarapu acknowledges funding from Bioscience Connecticut through Technology Translation Pipe-line program and University of Connecticut through SPARK technology commercialization program. Dr. Nukavarapu also acknowledges funding support from the National Institute of Biomedical Imaging and Bioengineering of the National Institutes of Health (Award Number R01EB020640). The authors acknowledge Katherine and Quinn for proof reading the manuscript.

References

1. Kumbar, SG., Laurencin, CT., Deng, M. Natural and Synthetic Biomedical Polymers. Oxford: Elsevier; 2014.
2. Gunatillake PA, Adhikari R. Biodegradable synthetic polymers for tissue engineering. Eur Cell Mater. 5:1–16. discussion 16, May 2003. [PubMed: 14562275]
3. Nukavarapu SP, Kumbar SG, Brown JL, Krogman NR, Weikel AL, Hindenlang MD, Nair LS, Allcock HR, Laurencin CT. Polyphosphazene/nano-hydroxyapatite composite microsphere scaffolds for bone tissue engineering. Biomacromolecules. Jul; 2008 9(7):1818–1825. [PubMed: 18517248]
4. Hutmacher DW. Scaffolds in tissue engineering bone and cartilage. Biomaterials. Dec; 2000 21(24): 2529–2543. [PubMed: 11071603]
5. Nukavarapu, SP., Freeman, J., Laurencin, CT. Regenerative Engineering of Musculoskeletal Tissues and Interfaces. Elsevier Science & Technology; 2015.
6. Amini AR, Adams DJ, Laurencin CT, Nukavarapu SP. Optimally porous and biomechanically compatible scaffolds for large-area bone regeneration. Tissue Eng Part A. Jul; 2012 18(13–14): 1376–1388. [PubMed: 22401817]
7. Amini AR, Xu TO, Chidambaram RM, Nukavarapu SP. Oxygen Tension- Controlled Matrices with Osteogenic and Vasculogenic Cells for Vascularized Bone Regeneration In Vivo. Tissue Eng Part A. Apr; 2016 22(7–8):610–620. [PubMed: 26914219]
8. Dorcemus DL, Nukavarapu SP. Novel and Unique Matrix Design for Osteochondral Tissue Engineering. MRS Online Proc Libr Arch. Jan.2014 1621:17–23.
9. Nukavarapu, SP., Liu, H., Deng, T., Oyen, M., Tamerler, C. Advances in Structure, Properties and Applications of Biological and Bioinspired Materials. Vol. 1621. Warrendale, PA: Materials Research Soceity;
10. Dorcemus DL, George EO, Dealy CN, Nukavarapu SP. Harnessing External Cues: Development and Evaluation of an In Vitro Culture System for Osteochondral Tissue Engineering. Tissue Eng Part A. Mar.2017
11. Amini AR, Laurencin CT, Nukavarapu SP. Bone tissue engineering: recent advances and challenges. Crit Rev Biomed Eng. 2012; 40(5):363–408. [PubMed: 23339648]
12. Nukavarapu, SP., Wallace, JS., Elgendy, HM., Liberman, JR., Laurencin, CT. An Introductions to Biomaterials and Their Applications. 2nd. CRC Press; 2011. Bone and biomaterials; p. 571-593.
13. Gentile P, Chiono V, Carmagnola I, Hatton PV. An overview of poly(lactic-co-glycolic) acid (PLGA)-based biomaterials for bone tissue engineering. Int J Mol Sci. Feb; 2014 15(3):3640–3659. [PubMed: 24590126]
14. Makadia HK, Siegel SJ. Poly Lactic-co-Glycolic Acid (PLGA) as Biodegradable Controlled Drug Delivery Carrier. Polymers. Aug; 2011 3(3):1377–1397. [PubMed: 22577513]
15. Ikada Y, Tsuji H. Biodegradable polyesters for medical and ecological applications. Macromol Rapid Commun. Feb; 2000 21(3):117–132.
16. Middleton JC, Tipton AJ. Synthetic biodegradable polymers as orthopedic devices. Biomaterials. Dec; 2000 21(23):2335–2346. [PubMed: 11055281]
17. Fu K, Pack DW, Klibanov AM, Langer R. Visual Evidence of Acidic Environment Within Degrading Poly(lactic-co-glycolic acid) (PLGA) Microspheres. Pharm Res. Jan; 2000 17(1):100–106. [PubMed: 10714616]

18. Pitt CG, Gratzl MM, Kimmel GL, Surles J, Schindler A. Aliphatic polyesters II. The degradation of poly (DL-lactide), poly (epsilon-caprolactone), and their copolymers in vivo. Biomaterials. Oct; 1981 2(4):215–220. [PubMed: 7326315]
19. Anderson JM, Shive MS. Biodegradation and biocompatibility of PLA and PLGA microspheres. Adv Drug Deliv Rev. Dec.2012 64:72–82.
20. Böstman O, Hirvensalo E, Mäkinen J, Rokkanen P. Foreign-body reactions to fracture fixation implants of biodegradable synthetic polymers. J Bone Joint Surg Br. Jul; 1990 72(4):592–596. [PubMed: 2199452]
21. Amini AR, Wallace JS, Nukavarapu SP. Short-term and long-term effects of orthopedic biodegradable implants. J Long Term Eff Med Implants. 2011; 21(2):93–122. [PubMed: 22043969]
22. Ehrenfried LM, Patel MH, Cameron RE. The effect of tri-calcium phosphate (TCP) addition on the degradation of polylactide-co-glycolide (PLGA). J Mater Sci Mater Med. Jan; 2008 19(1):459–466. [PubMed: 17607516]
23. Yang Y, Zhao Y, Tang G, Li H, Yuan X, Fan Y. In vitro degradation of porous poly(l-lactide-co-glycolide)/β-tricalcium phosphate (PLGA/β-TCP) scaffolds under dynamic and static conditions. Polym Degrad Stab. Oct; 2008 93(10):1838–1845.
24. Kim SS, Sun Park M, Jeon O, Yong Choi C, Kim B. Poly(lactide-co-glycolide)/hydroxyapatite composite scaffolds for bone tissue engineering. Biomaterials. Mar; 2006 27(8):1399–1409. [PubMed: 16169074]
25. Higashi S, Yamamuro T, Nakamura T, Ikada Y, Hyon SH, Jamshidi K. Polymer-hydroxyapatite composites for biodegradable bone fillers. Biomaterials. May; 1986 7(3):183–187. [PubMed: 3013326]
26. Deng M, Nair LS, Nukavarapu SP, Kumbar SG, Jiang T, Krogman NR, Singh A, Allcock HR, Laurencin CT. Miscibility and in vitro osteocompatibility of biodegradable blends of poly[(ethyl alanato) (p-phenyl phenoxy) phosphazene] and poly(lactic acid-glycolic acid). Biomaterials. Jan; 2008 29(3):337–349. [PubMed: 17942150]
27. Deng M, Nair LS, Nukavarapu SP, Kumbar SG, Jiang T, Weikel AL, Krogman NR, Allcock HR, Laurencin CT. In Situ Porous Structures: A Unique Polymer Erosion Mechanism in Biodegradable Dipeptide-based Polyphosphazene and Polyester Blends Producing Matrices for Regenerative Engineering. Adv Funct Mater. Sep; 2010 20(17):2743–2957. [PubMed: 21789036]
28. Deng M, Nair LS, Nukavarapu SP, Jiang T, Kanner WA, Li X, Kumbar SG, Weikel AL, Krogman NR, Allcock HR, Laurencin CT. Dipeptide-based polyphosphazene and polyester blends for bone tissue engineering. Biomaterials. Jun; 2010 31(18):4898–4908. [PubMed: 20334909]
29. Krogman NR, Weikel AL, Kristhart KA, Nukavarapu SP, Deng M, Nair LS, Laurencin CT, Allcock HR. The influence of side group modification in polyphosphazenes on hydrolysis and cell adhesion of blends with PLGA. Biomaterials. Jun; 2009 30(17):3035–3041. [PubMed: 19345410]
30. Deng M, Nair LS, Nukavarapu SP, Kumbar SG, Brown JL, Krogman NR, Weikel AL, Allcock HR, Laurencin CT. Biomimetic, bioactive etheric polyphosphazene-poly(lactide-co-glycolide) blends for bone tissue engineering. J Biomed Mater Res A. Jan; 2010 92(1):114–125. [PubMed: 19165780]
31. Zheng YF, Gu XN, Witte F. Biodegradable metals. Mater Sci Eng R Rep. Mar; 2014 77(Supplement C):1–34.
32. Staiger MP, Pietak AM, Huadmai J, Dias G. Magnesium and its alloys as orthopedic biomaterials: a review. Biomaterials. Mar; 2006 27(9):1728–1734. [PubMed: 16246414]
33. Alvarez K, Nakajima H. Metallic Scaffolds for Bone Regeneration. Materials. Jul; 2009 2(3):790–832.
34. Hort N, Huang Y, Fechner D, Störmer M, Blawert C, Witte F, Vogt C, Drücker H, Willumeit R, Kainer KU, Feyerabend F. Magnesium alloys as implant materials – Principles of property design for Mg–RE alloys. Acta Biomater. May; 2010 6(5):1714–1725. [PubMed: 19788945]
35. Farraro KF, Kim KE, Woo SLY, Flowers JR, McCullough MB. Revolutionizing orthopaedic biomaterials: The potential of biodegradable and bioresorbable magnesium-based materials for functional tissue engineering. J Biomech. Jun; 2014 47(9):1979–1986. [PubMed: 24373510]

36. Landi E, Logroscino G, Proietti L, Tampieri A, Sandri M, Sprio S. Biomimetic Mg-substituted hydroxyapatite: from synthesis to in vivo behaviour. J Mater Sci Mater Med. Jan; 2008 19(1):239–247. [PubMed: 17597369]
37. Witte F, Fischer J, Nellesen J, Crostack HA, Kaese V, Pisch A, Beckmann F, Windhagen H. In vitro and in vivo corrosion measurements of magnesium alloys. Biomaterials. Mar; 2006 27(7):1013–1018. [PubMed: 16122786]
38. Gu XN, Zheng YF. A review on magnesium alloys as biodegradable materials. Front Mater Sci China. Jun; 2010 4(2):111–115.
39. ASTM D882-12, Standard Test Method for Tensile Properties of Thin Plastic Sheeting. ASTM International; West Conshohocken, PA: 2012.
40. Agrawal CM, Huang D, Schmitz JP, Athanasiou KA. Elevated Temperature Degradation of a 50:50 Copolymer of PLA-PGA. Tissue Eng. Dec; 1997 3(4):345–352.
41. Zolnik BS, Leary PE, Burgess DJ. Elevated temperature accelerated release testing of PLGA microspheres. J Controlled Release. May; 2006 112(3):293–300.
42. Alexis F. Factors affecting the degradation and drug-release mechanism of poly(lactic acid) and poly[(lactic acid)-co-(glycolic acid)]. Polym Int. Jan; 2005 54(1):36–46.
43. Tanahashi M, Yao T, Kokubo T, Minoda M, Miyamoto T, Nakamura T, Yamamuro T. Apatite Coating on Organic Polymers by a Biomimetic Process. J Am Ceram Soc. Nov; 1994 77(11): 2805–2808.
44. Kokubo T, Kushitani H, Sakka S, Kitsugi T, Yamamuro T. Solutions able to reproduce in vivo surface-structure changes in bioactive glass-ceramic A-W3. J Biomed Mater Res. Jun; 1990 24(6): 721–734. [PubMed: 2361964]
45. Igwe JC, Mikael PE, Nukavarapu SP. Design, fabrication and in vitro evaluation of a novel polymer-hydrogel hybrid scaffold for bone tissue engineering. J Tissue Eng Regen Med. Feb; 2014 8(2):131–142. [PubMed: 22689304]
46. Yoshizawa S, Brown A, Barchowsky A, Sfeir C. Magnesium ion stimulation of bone marrow stromal cells enhances osteogenic activity, simulating the effect of magnesium alloy degradation. Acta Biomater. Jun; 2014 10(6):2834–2842. [PubMed: 24512978]
47. Zhang E, Xu L, Yu G, Pan F, Yang K. In vivo evaluation of biodegradable magnesium alloy bone implant in the first 6 months implantation. J Biomed Mater Res A. Sep; 2009 90A(3):882–893.
48. Witte F, Kaese V, Haferkamp H, Switzer E, Meyer-Lindenberg A, Wirth CJ, Windhagen H. In vivo corrosion of four magnesium alloys and the associated bone response. Biomaterials. Jun; 2005 26(17):3557–3563. [PubMed: 15621246]
49. Ahmed S, Jones FR. A review of particulate reinforcement theories for polymer composites. J Mater Sci. Dec; 1990 25(12):4933–4942.
50. Mikael PE, Amini AR, Basu J, Josefina Arellano-Jimenez M, Laurencin CT, Sanders MM, Barry Carter C, Nukavarapu SP. Functionalized carbon nanotube reinforced scaffolds for bone regenerative engineering: fabrication, in vitro and in vivo evaluation. Biomed Mater Bristol Engl. Jun.2014 9(3):035001.
51. Mikael P, Nukavarapu S. Functionalized Carbon Nanotube Composite Scaffolds for Bone Tissue Engineering: Prospects and Progress. J Biomater Tissue Eng. Jun.2011 1:76–85.
52. Zolnik BS, Burgess DJ. Effect of acidic pH on PLGA microsphere degradation and release. J Control Release Off J Control Release Soc. Oct; 2007 122(3):338–344.
53. Lu L, Garcia CA, Mikos AG. In vitro degradation of thin poly(DL-lactic-co-glycolic acid) films. J Biomed Mater Res. Aug; 1999 46(2):236–244. [PubMed: 10380002]
54. Grizzi I, Garreau H, Li S, Vert M. Hydrolytic degradation of devices based on poly(dl-lactic acid) size-dependence. Biomaterials. Mar; 1995 16(4):305–311. [PubMed: 7772670]
55. Park TG. Degradation of poly(lactic-co-glycolic acid) microspheres: effect of copolymer composition. Biomaterials. Oct; 1995 16(15):1123–1130. [PubMed: 8562787]
56. Kokubo T, Takadama H. How useful is SBF in predicting in vivo bone bioactivity? Biomaterials. May; 2006 27(15):2907–2915. [PubMed: 16448693]
57. Li L, Gao J, Wang Y. Evaluation of cyto-toxicity and corrosion behavior of alkali-heat-treated magnesium in simulated body fluid. Surf Coat Technol. Jul; 2004 185(1):92–98.

58. Kuwahara H, Al-Abdullat Y, Mazaki N, Tsutsumi S, Aizawa T. Precipitation of magnesium apatite on pure magnesium surface during immersing in Hank's solution. Mater Trans. 2001; 42(7):1317–1321.

59. Xu L, Yu G, Zhang E, Pan F, Yang K. In vivo corrosion behavior of Mg-Mn-Zn alloy for bone implant application. J Biomed Mater Res A. Dec; 2007 83A(3):703–711.

60. Brown A, Zaky S, Ray H, Sfeir C. Porous magnesium/PLGA composite scaffolds for enhanced bone regeneration following tooth extraction. Acta Biomater. Jan; 2015 11(Supplement C):543–553. [PubMed: 25234156]

61. Janning C, Willbold E, Vogt C, Nellesen J, Meyer-Lindenberg A, Windhagen H, Thorey F, Witte F. Magnesium hydroxide temporarily enhancing osteoblast activity and decreasing the osteoclast number in peri-implant bone remodelling. Acta Biomater. May; 2010 6(5):1861–1868. [PubMed: 20035905]

62. Dvorak MM, Riccardi D. Ca2+ as an extracellular signal in bone. Cell Calcium. Mar; 2004 35(3): 249–255. [PubMed: 15200148]

63. Dvorak MM, Siddiqua A, Ward DT, Carter DH, Dallas SL, Nemeth EF, Riccardi D. Physiological changes in extracellular calcium concentration directly control osteoblast function in the absence of calciotropic hormones. Proc Natl Acad Sci U S A. Apr; 2004 101(14):5140–5145. [PubMed: 15051872]

64. Nakamura S, Matsumoto T, Sasaki JI, Egusa H, Lee KY, Nakano T, Sohmura T, Nakahira A. Effect of Calcium Ion Concentrations on Osteogenic Differentiation and Hematopoietic Stem Cell Niche-Related Protein Expression in Osteoblasts. Tissue Eng Part A. Mar; 2010 16(8):2467–2473. [PubMed: 20214455]

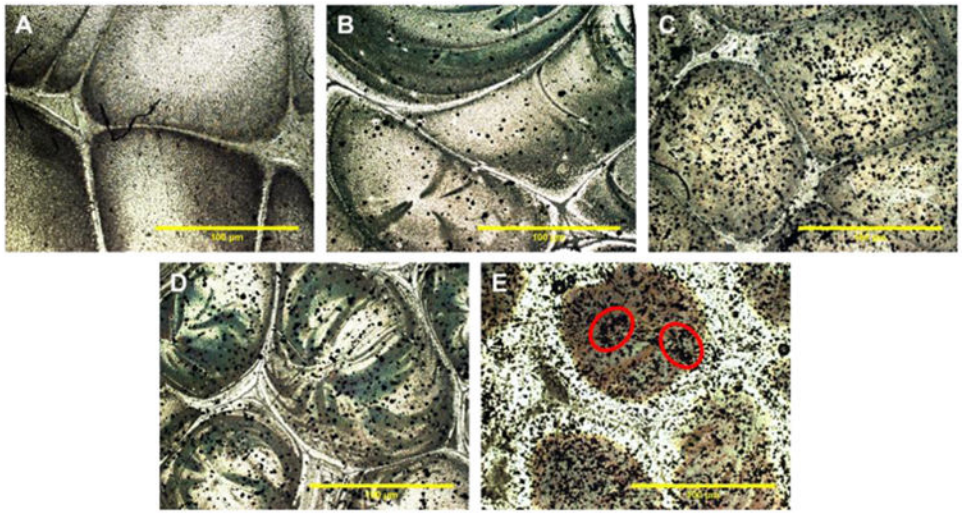

Figure 1.

Magnesium particle dispersion in PLGA-Mg composite films. Representative optical micrographs of (A) PLGA only, and PLGA-Mg composites with (B) 1 wt% Mg, (C) 3 wt% Mg, (D) 5 wt% Mg, and (E) 10 wt% Mg. Mg particles, seen in black, are evenly dispersed throughout the film in concentration ranging from 0-5 wt%. Traces of Mg particle agglomeration was seen in PLGA-Mg composite films with 10wt% of Mg (circled regions in E show Mg particle agglomeration).

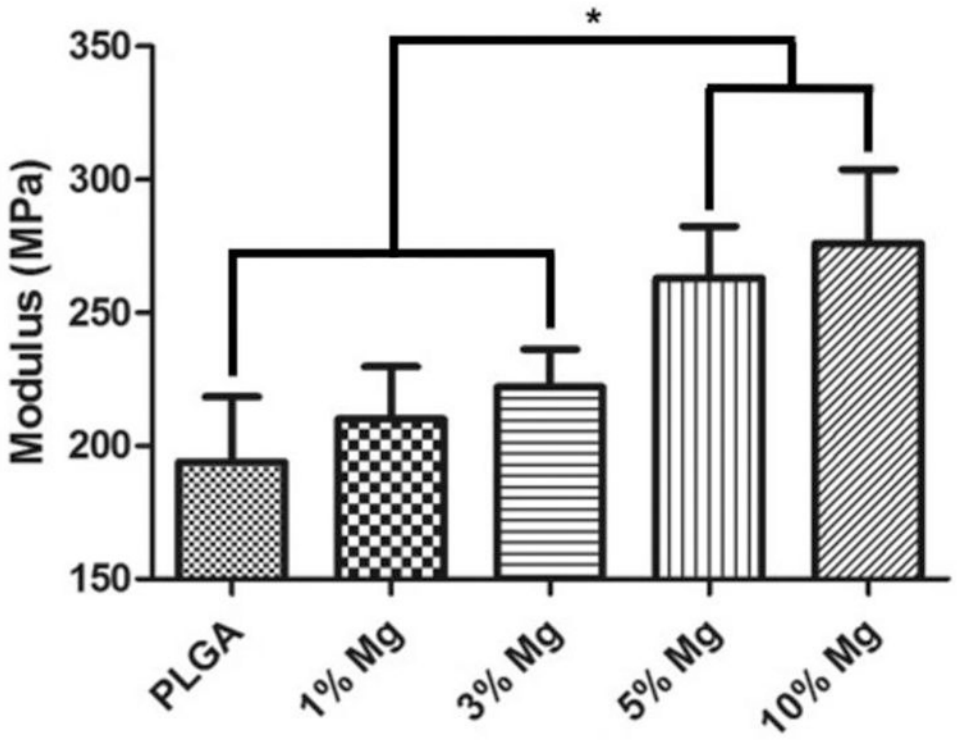

Figure 2.

Effect of Mg loading on tensile modulus of the composite films. PLGA-Mg composite films with varying Mg wt% loading were subjected for mechanical strength measurement in tensile mode. An increase in tensile modulus of the composites was seen with increase in Mg loading. The increase in the modulus is statistically significant for the composite groups of 3 and 5 wt% of Mg (n=6; * = $p < 0.05$).

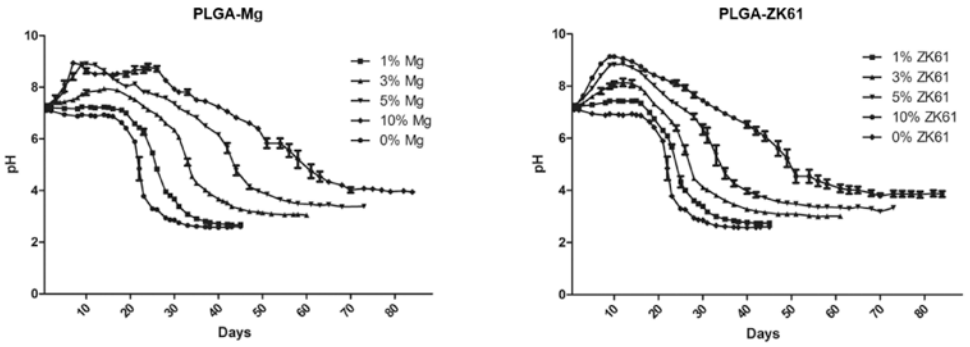

Figure 3.

In vitro degradation profile of composite films. PLGA-Mg films of different Mg concentrations were subjected to degradation at elevated temperature 47 C in PBS. (A) degradation profile of composites using pure Mg particles. (B) Degradation profile of films containing with the Zn-Mg alloy ZK61. For both pure Mg and Zn-Mg alloys, near neutral or above pH 7 conditions were maintained for longer than the pure PLGA samples and extended the duration of degradation. Initial increase in pH was also observed in samples containing Mg or ZK61 alloy, that varied in intensity relative to the concentration of Mg or Zn-Mg alloy.

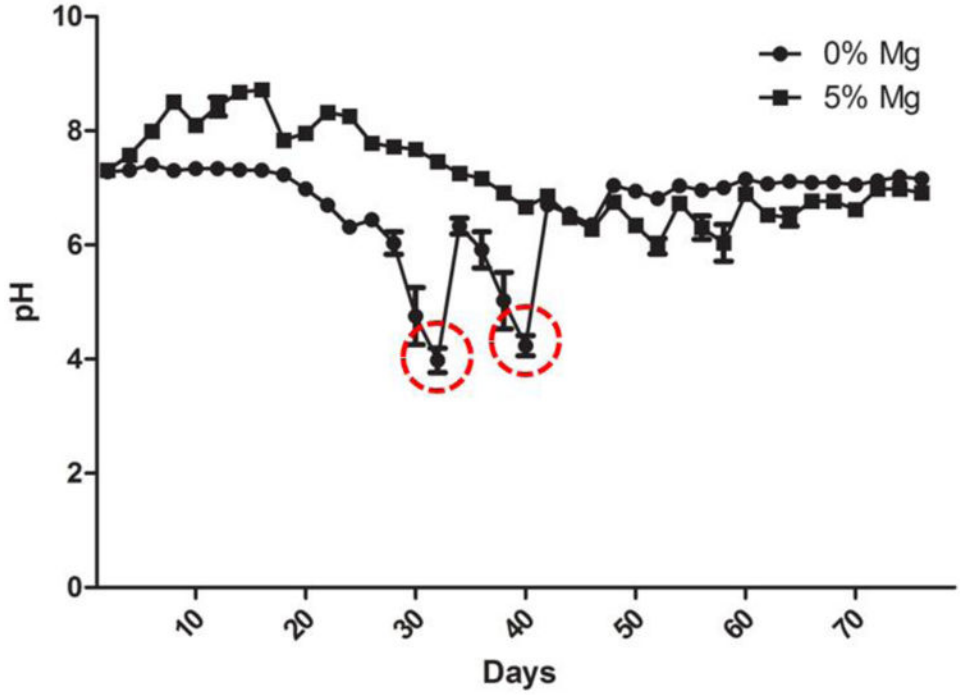

Figure 4.

Dynamic or sink condition degradation profile of PLGA-Mg films. *In vivo* fluid clearance is simulated *in vitro* for the degradation of the PLGA-Mg composites at 47 C in PBS. Degradation media was changed every 7 days to simulate the normal sink conditions in vivo. The PLGA-Mg composites displayed a steady near neutral conditions throughout the duration of the study. The PLGA alone group displayed sharp decreases in pH (highlighted within red circles).

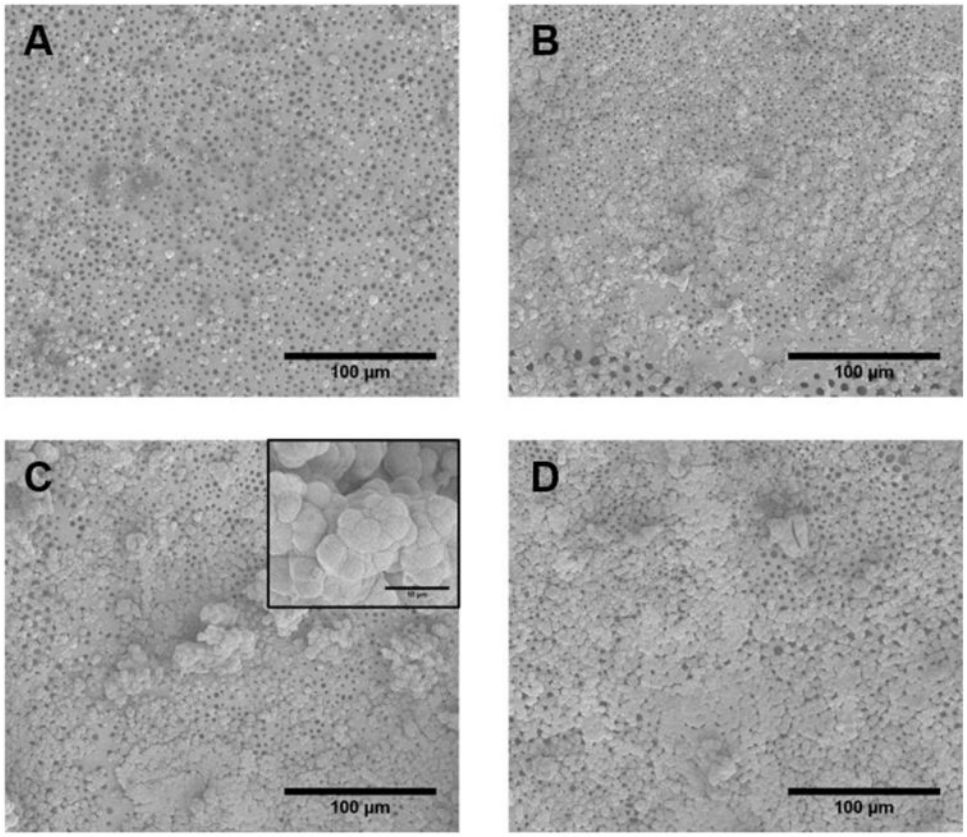

Figure 5.

In vitro biomineralization of the PLGA-Mg composites. The samples were immersed in 1.5 × for 14 days. Representative SEM micrographs show the deposited biomineral for (A) PLGA, and (B-D) for composites with Mg content of 1, 3, and 5 wt%, respectively. Insert in C shows representative close-up of apatite nucleates (Scale bar 10 μM). PLGA sample showed small isolated nucleation of calcium apatite. The amount of apatite nucleation increased with Mg concentration in composites, with 5 wt% samples displaying the greatest amount of apatite nucleates with greater amount of surface coverage.

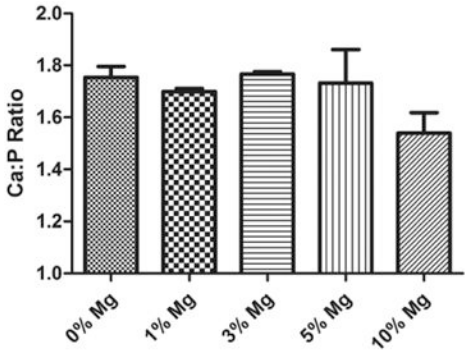

Mg Wt%	Mean Ca:P Ratio ± Std. Dev.
0	1.699 ± 0.042
1	1.699 ± 0.012
3	1.766 ± 0.009
5	1.732 ± 0.130
10	1.539 ± 0.078

Figure 6.

Biomineral composition and Ca to P ratio analysis. Mean Ca to P atomic ratio was obtained from EDS analysis of the precipitates on the composite films. PLGA and PLGA-Mg samples showed similar Ca:P ratio and did not differ with the amount of Mg loading. (n=3).

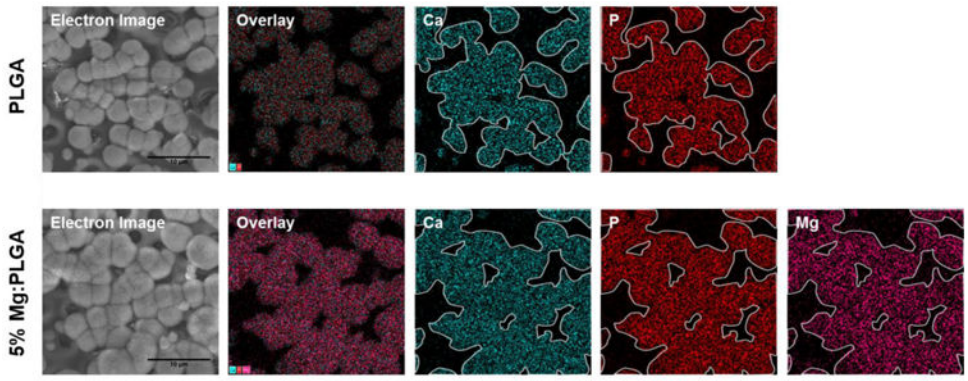

Figure 7.

Effect of Mg composition on *in vitro* biomineralization. EDS elemental analysis of the PLGA and PLGA-Mg composites after 14 day immersion in 1.5× SBF. The presence of Ca (outlined in white and overlaid in other groups) and P groups were detected in the nucleates for both polymer and composite groups, indicating formation of calcium apatite. The precipitation of calcium apatite coincided with the presence of Mg in the PLGA-Mg composite films, indicating a relationship between the increased local Mg concentration and the calcium apatite nucleation and growth.

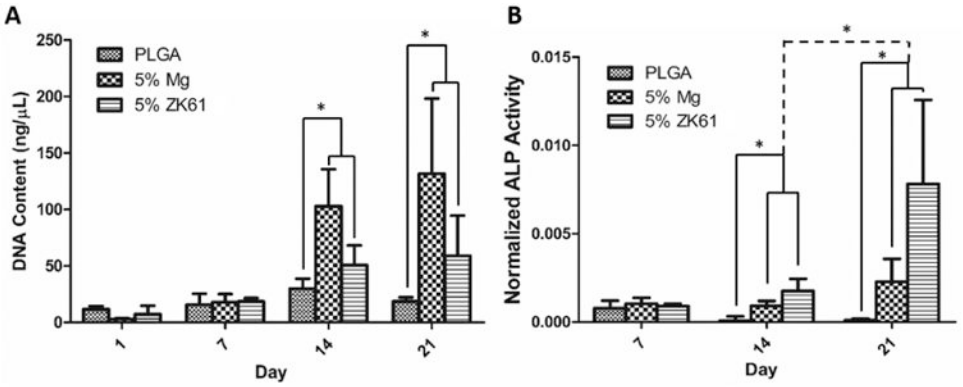

Figure 8.

In vitro biocompatibility. Mouse pre-osteoblastic (MC3T3-E1) cell performance and osteogenic differentiation on PLGA, PLGA-Mg, and PLGA-ZK61 was assessed through DNA quantification and ALP expression. (A) Cellular proliferation was analyzed using Picogreen dsDNA assay. Increased cell proliferation for Mg and ZK61 samples was observed at days 14 and 21, with little change in DNA concentration in PLGA group throughout the study. (B) ALP expression was analyzed using an ALP assay kit and normalized to DNA concentration. Increased ALP expression was seen between PLGA and the composite groups at days 14 and 21. Significant increase in ALP expression between day 14 and 21 was also seen for the PLGA-Mg and PLGA-ZK61 samples (n=3* = $p < 0.05$).

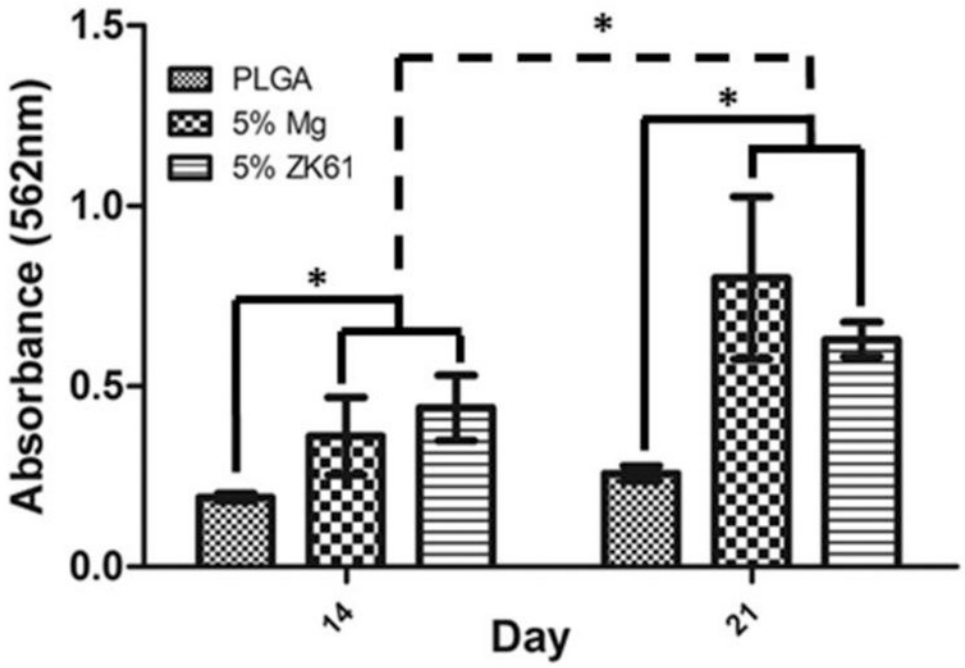

Figure 9.

In vitro mineralization via Alizarin red staining and quantification. MC3T3-E1 pre-osteoblastic cell induced mineralization for the PLGA and PLGA-Mg composite groups after 14 and 21 days *in vitro*. Mg or ZK61 alloy composite groups displayed significant increases in mineral formation in comparison to PLGA alone group at 14 and 21 days. The PLGA-Mg and PLGA-ZK61 samples also showed significant increase in mineralization between day 14 and 21 (n=3* = $p<0.05$).